

Magnetic and thermal properties of the $S = 1/2$ zig-zag spin-chain compound In_2VO_5

Yogesh Singh, R. W. McCallum, and D. C. Johnston

Ames Laboratory and Department of Physics and Astronomy, Iowa State University, Ames, IA 50011

(Dated: February 1, 2008)

Static magnetic susceptibility χ , ac susceptibility χ_{ac} and specific heat C versus temperature T measurements on polycrystalline samples of In_2VO_5 and χ and C versus T measurements on the isostructural, nonmagnetic compound In_2TiO_5 are reported. A Curie-Weiss fit to the $\chi(T)$ data above 175 K for In_2VO_5 indicates ferromagnetic exchange between V^{4+} ($S = 1/2$) moments. Below 150 K the $\chi(T)$ data deviate from the Curie-Weiss behavior but there is no signature of any long range magnetic order down to 1.8 K. There is a cusp at 2.8 K in the zero field cooled (ZFC) $\chi(T)$ data measured in a magnetic field of 100 Oe and the ZFC and field cooled (FC) data show a bifurcation below this temperature. The frequency dependence of the $\chi_{ac}(T)$ data indicate that below 3 K the system is in a spin-glass state. The difference ΔC between the heat capacity of In_2VO_5 and In_2TiO_5 shows a broad anomaly peaked at 130 K. The entropy upto 300 K is more than what is expected for $S = 1/2$ moments. The anomaly in ΔC and the extra entropy suggests that there may be a structural change below 130 K in In_2VO_5 .

I. INTRODUCTION

Quasi-one dimensional spin-chain and spin-ladder materials have been studied partly in the hope of understanding the physics of the high T_c parent compounds¹ which can be viewed as an infinite array of spin-ladders in a plane, and also for the unusual quantum magnetism that these materials themselves exhibit. For example, the spin-Peierls state in CuGeO_3 ($S = 1/2$),² the spin gap in the two-leg ladder system SrCu_2O_3 ($S = 1/2$),³ and the Haldane gap in Y_2BaNiO_5 ($S = 1$)⁴ to name a few. Holes doped into these quasi-two-dimensional ladders have also been predicted to pair and superconduct.⁵ Frustration in addition to the low dimensionality leads to further exotic properties like the Wigner crystallization of magnons in the quasi-two-dimensional material $\text{SrCu}_2(\text{BO}_3)_2$,⁶ partial antiferromagnetic ordering in the spin chain materials $\text{Sr}_5\text{Rh}_4\text{O}_{12}$, $\text{Ca}_5\text{Ir}_3\text{O}_{12}$ and Ca_4IrO_6 ,⁷ and order by disorder phenomena in the frustrated spin-chain compound $\text{Ca}_3\text{Co}_2\text{O}_6$.⁸

Recently based on crystal chemical analysis, the orthorhombic ($Pnma$) compound In_2VO_5 has been proposed to be a $S = 1/2$ zig-zag spin chain compound with competing nearest (J_1) and next nearest neighbor (J_2) antiferromagnetic exchange couplings between V^{4+} moments.⁹ The compound In_2VO_5 was first prepared both in polycrystalline and single crystalline form by Senegas and the single crystal structure was reported.¹⁰ The crystal structure is shown in Fig. 1. Figure 1(a) shows the zig-zag vanadium chains extending along the b -axis with nearest and next-nearest neighbor exchanges J_1 and J_2 respectively, and Fig. 1(b) shows the structure along the b -axis showing the arrangement of the chains in the ac -plane. The V atoms are crystallographically equivalent at room temperature.¹⁰ A crystal chemical analysis estimated antiferromagnetic J_1 and J_2 with $J_2/J_1 = 1.68$.⁹ Recent band structure calculations showed, however, that the room temperature crystal structure was incompatible with antiferromagnetic interactions and claimed that both J_1 and J_2 should be

ferromagnetic instead.¹¹ Apart from the synthesis and crystal structure, an experimental study of the physical properties of this material have not been reported before.

Herein we report the magnetic and thermal properties of In_2VO_5 and the isostructural nonmagnetic compound In_2TiO_5 . The static magnetic susceptibility χ , the ac susceptibility χ_{ac} and the heat capacity C versus temperature T measurements on the compound In_2VO_5 and χ and C versus T measurements on the compound In_2TiO_5 are reported. Our results indicate predominantly ferromagnetic exchange interactions between V^{4+} moments above 150 K. The product χT versus T shows a sudden reduction below about 120 K. There is no signature of long-range magnetic ordering down to 1.8 K. Surprisingly the $\chi(T)$ data, $\chi_{ac}(T)$ at various frequencies and the $C(T)$ data suggest that stoichiometric In_2VO_5 undergoes a transition into a spin-glass state below about 3 K. The difference ΔC between the heat capacities of In_2VO_5 and In_2TiO_5 shows a well-defined peak at 130 K and the entropy difference ΔS obtained by integrating the $\Delta C/T$ versus T data up to 300 K is much larger than the value expected for $S = 1/2$ moments. The peak in ΔC and the extra entropy suggest a structural change in In_2VO_5 below ~ 130 K.

II. EXPERIMENTAL DETAILS

Polycrystalline samples of In_2VO_5 and In_2TiO_5 were prepared by solid state synthesis. The starting materials used were In_2O_3 (99.99%, JMC), V_2O_3 (99.995%, MV labs), V_2O_5 (99.995%, MV Labs) and TiO_2 (99.999%, MV labs). Samples of In_2VO_5 were prepared by the reaction of In_2O_3 and VO_2 at 1100 °C for 72 hrs in sealed quartz tubes with intermediate grindings after every 24 hrs. The VO_2 was prepared by the reaction of equimolar quantities of the above V_2O_3 and V_2O_5 in a sealed quartz tube with an initial firing of 24 hrs at 900 °C and a second firing of 24 hrs at 1000 °C. Samples of In_2TiO_5 were prepared by the reaction of stoichiomet-

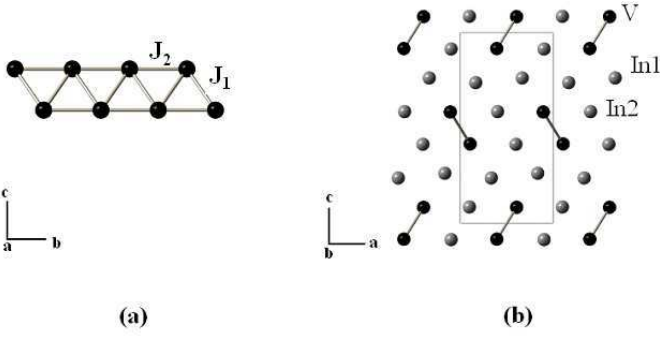


FIG. 1: (a) A segment of the crystal structure of In_2VO_5 along the a -axis showing the zig-zag chains of V^{4+} moments along the b -axis with nearest neighbor (J_1) and next-nearest neighbor (J_2) exchange interactions. (b) The crystal structure along the b -axis showing the arrangement of the chains in the ac -plane.

ric quantities of In_2O_3 and TiO_2 at 1200°C for 72 hrs in air with intermediate grindings after every 24 hrs. Hard well-sintered pellets were obtained. Part of the pellet was crushed for powder x-ray diffraction (XRD). The XRD patterns were obtained at room temperature using a Rigaku Geigerflex diffractometer with $\text{Cu K}\alpha$ radiation, in the 2θ range from 10 to 90° with a 0.02° step size. Intensity data were accumulated for 5 s per step. The $\chi(T)$ and $\chi_{ac}(T)$ were measured using a commercial Superconducting Quantum Interference Device (SQUID) magnetometer (MPMS5, Quantum Design) and the $C(T)$ was measured using a commercial Physical Property Measurement System (PPMS5, Quantum Design).

III. RESULTS

A. Structure of In_2VO_5 and In_2TiO_5

All the lines in the X-ray patterns of In_2VO_5 and In_2TiO_5 could be indexed to the known¹⁰ orthorhombic $Pnma$ (No. 166) structure and Rietveld refinements,¹² shown in Fig. 2, of the X-ray patterns gave the lattice parameters $a = 7.2282(5) \text{ \AA}$, $b = 3.4462(2) \text{ \AA}$ and $c = 14.827(1) \text{ \AA}$ for In_2VO_5 , and $a = 7.2419(9) \text{ \AA}$, $b = 3.5031(4) \text{ \AA}$ and $c = 14.892(2) \text{ \AA}$ for In_2TiO_5 . These values are in reasonable agreement with previously reported values for In_2VO_5 ($a = 7.232 \text{ \AA}$, $b = 3.468 \text{ \AA}$ and $c = 14.82 \text{ \AA}$) and In_2TiO_5 ($a = 7.237 \text{ \AA}$, $b = 3.429 \text{ \AA}$ and $c = 14.86 \text{ \AA}$).¹⁰ Some parameters obtained from the Rietveld refinements of our samples are given in Table I.

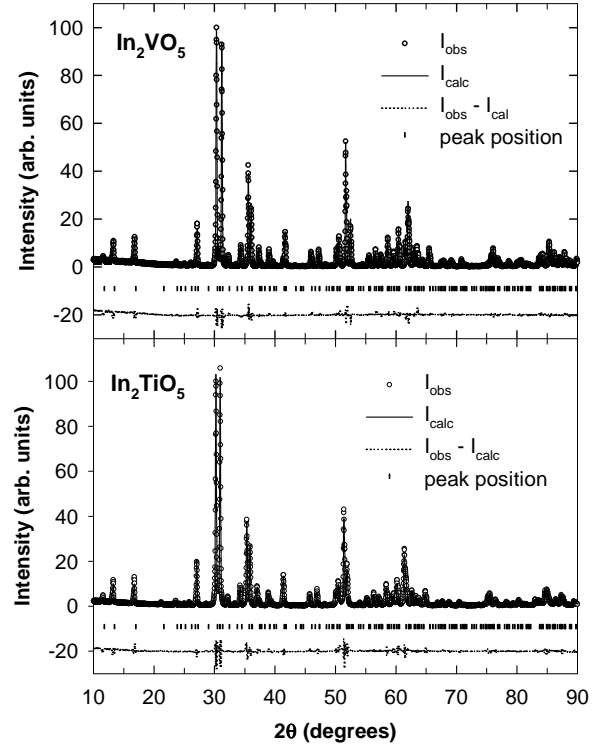


FIG. 2: Rietveld refinements of the In_2VO_5 and In_2TiO_5 X-ray diffraction data. The open symbols represent the observed data, the solid lines represent the fitted pattern, the dotted lines represent the difference between the observed and calculated intensities and the vertical bars represent the peak positions.

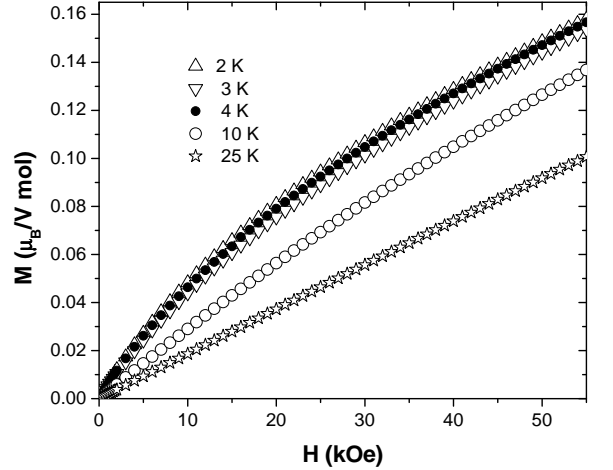


FIG. 3: Isothermal magnetization M versus magnetic field H at various temperatures for In_2VO_5 .

B. Magnetization Measurements

1. Isothermal Magnetization versus Magnetic Field

Figure 3 shows the isothermal magnetization M versus magnetic field H measured at various temperatures T .

TABLE I: Structure parameters for In_2VO_5 and In_2TiO_5 refined from powder XRD data. The overall isotropic thermal parameter B is defined within the temperature factor of the intensity as $e^{-2B \sin^2 \theta / \lambda^2}$.

Sample	atom	x	y	z	B (\AA^2)	R_{wp}	R_{p}
In_2VO_5	In	0.0967(7)	0.25	0.0851(2)	0.003(1)	0.224	0.154
	In	0.3320(6)	0.75	0.2374(2)	0.006(1)		
	V	0.110(2)	0.25	0.4194(7)	0.013(3)		
	O	0.249(3)	0.25	0.308(2)	0.006(9)		
	O	0.339(3)	0.25	0.502(2)	0.009(9)		
	O	0.364(3)	0.25	0.155(1)	0.013(8)		
	O	0.057(3)	0.75	0.180(1)	0.026(7)		
	O	0.071(4)	0.75	0.449(2)	0.03(1)		
In_2VO_5	In	0.097(5)	0.25	0.0852(2)	0.008(1)	0.195	0.139
	In	0.3294(5)	0.75	0.2389(2)	0.006(1)		
	Ti	0.1098(12)	0.25	0.4216(6)	0.023(3)		
	O	0.245(3)	0.25	0.315(1)	0.002(6)		
	O	0.350(3)	0.25	0.495(2)	0.018(8)		
	O	0.362(2)	0.25	0.156(2)	0.03(1)		
	O	0.061(3)	0.75	0.180(1)	0.016(9)		
	O	0.066(3)	0.75	0.447(2)	0.035(9)		

The $M(H)$ data at 25 K and at higher temperatures (not shown) are linear. Below 10 K, however, the $M(H)$ data show a negative curvature at low fields with no sign of saturation even at the highest field $H = 55$ kOe. The $M(H)$ data could not be fitted by a Brillouin function assuming $S = 1/2$ and $g = 2$ or any other reasonable value of S ($S = 1$ for example). The reason can be seen from the data in Fig. 3 for $T = 2, 3$, and 4 K, which are nearly the same despite the factor of two range in temperature. This indicates that the curvature in the $M(H)$ data is not due to the presence of nearly isolated paramagnetic impurities in the sample. The negative curvature in Fig. 3 may be associated with the spin-glass like state that we infer from our magnetic susceptibility and heat capacity data that we discuss below for In_2VO_5 .

2. Magnetic Susceptibility

The temperature dependence of the magnetic susceptibility $\chi \equiv M/H$ between 1.8 K and 400 K for In_2VO_5 measured in an applied magnetic field $H = 1$ T is shown in the main panel of Fig. 4(a). The inset in Fig. 4(a) shows the zero-field-cooled (ZFC) and field-cooled (FC) χ data between 1.8 K and 8 K measured in an applied magnetic field $H = 100$ Oe. The ZFC data show a cusp at 2.8 K and the ZFC data and FC data bifurcate below this temperature. This feature is suggestive of a spin-glass state and we will return to these data when we discuss the ac susceptibility data below. Figure 4(b) shows the $\chi^{-1}(T)$ data between 1.8 K and 400 K. The $\chi(T)$ data between 175 K and 400 K were fitted by the Curie-Weiss

expression $\chi = \chi_0 + C/(T - \theta)$ and the fit, shown as the solid curve through the $\chi^{-1}(T)$ data in Fig. 4(b) and extrapolated to lower temperatures (dashed curve), gave $\chi_0 = -5.5(8) \times 10^{-5} \text{ cm}^3/\text{mol}$, $C = 0.386(7) \text{ cm}^3 \text{ K/mol}$ and $\theta = 26(2) \text{ K}$. The value of C corresponds to an effective moment of $1.75(2) \mu_B/\text{V}$ which is close to the value ($1.73 \mu_B/\text{V}$) expected for $S = 1/2$ moments with a g -factor of 2. The positive value for θ indicates that the dominant interactions between the V^{4+} moments are ferromagnetic. This supports the results of the band structure calculations.¹¹ The $\chi^{-1}(T)$ data deviate from the Curie-Weiss behavior below 150 K, showing an upward curvature. The $\chi^{-1}(T)$ decreases again below about 5 K which corresponds to the temperature of the cusp in the χ data in the inset of Fig. 4(a). The inset in Fig. 4(b) shows the χT versus T data showing a pronounced reduction below about 120 K where the $\chi(T)$ data deviate from the Curie-Weiss law.

Let us now return to the low field $\chi(T)$ data in the inset of Fig. 4(a). The cusp in the ZFC χ data and the bifurcation between the ZFC and FC susceptibility suggests spin-glass freezing with a freezing temperature $T_f = 2.8$ K. To check this possibility we have measured the ac susceptibility χ_{ac} at various frequencies around the temperature of the cusp. The real χ'_{ac} and imaginary χ''_{ac} parts of the χ_{ac} data between 2 K and 4 K, measured in an ac field of 1 Oe and with various drive frequencies, are shown in Figs. 5(a) and (b). The maximum in the χ'_{ac} data at 1 Hz occurs at 2.76 K and monotonically moves up in temperature with increasing frequency. This trend is also seen in the χ''_{ac} data. The low field χ data in the inset of Fig. 4(a) and the χ_{ac} data in Figs. 5(a) and

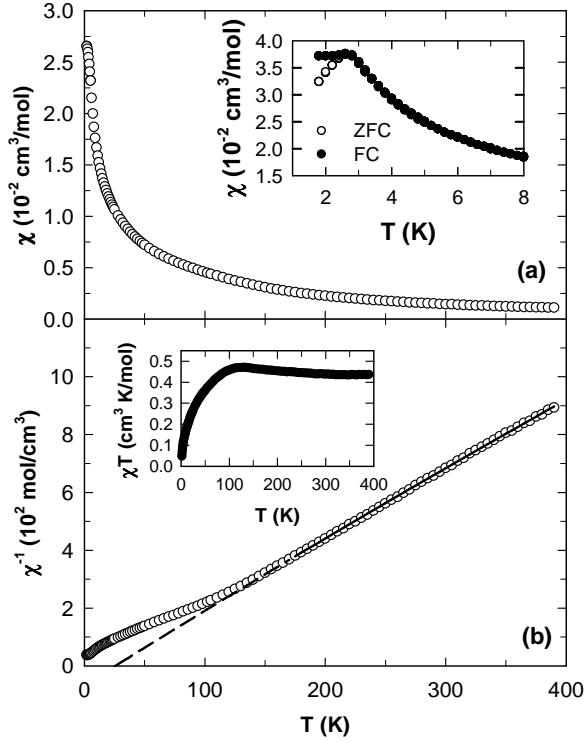


FIG. 4: (a) The magnetic susceptibility χ versus temperature T for In_2VO_5 measured with an applied magnetic field of 1 T. The inset in (a) shows the zero field cooled (ZFC) and field cooled (FC) $\chi(T)$ data measured in an applied magnetic field of 100 Oe. (b) The inverse susceptibility χ^{-1} versus temperature T data (symbols) and a fit by a Curie-Weiss model (solid line) extrapolated to lower temperatures (dashed line). The inset in (b) shows the χT versus T data revealing a sudden reduction below about 120 K.

(b), together with the absence of a noticeable anomaly at T_f in the heat capacity data discussed below, are features usually observed at a spin-glass transition¹³ and strongly point to the existence of a spin-glass state below $T_f = 2.8$ K in In_2VO_5 .

The magnetic susceptibility χ versus temperature T for the isostructural and nominally nonmagnetic compound In_2TiO_5 is shown as open symbols in Fig. 6. The $\chi(T)$ is negative and almost temperature independent in the whole temperature range except for a small upturn at low temperatures. The $\chi(T)$ data in the whole temperature range was fitted by a Curie-Weiss expression $\chi = \chi_0 + C/(T - \theta)$. The fit, shown in Fig. 6 as the solid curve through the data, gave the values $\chi_0 = -1.33(1) \times 10^{-4}$ cm³/mol, $C = 8.13(2) \times 10^{-4}$ cm³/mol (corresponding to about 4 mol% spin-1/2 impurities) and $\theta = -1.60(5)$ K. The value of χ_0 is of the same order as the core susceptibility $\chi_{\text{core}} = -1.0 \times 10^{-4}$ cm³/mol obtained from the sum of the atomic diamagnetic susceptibilities¹⁴ of the atoms in the material.

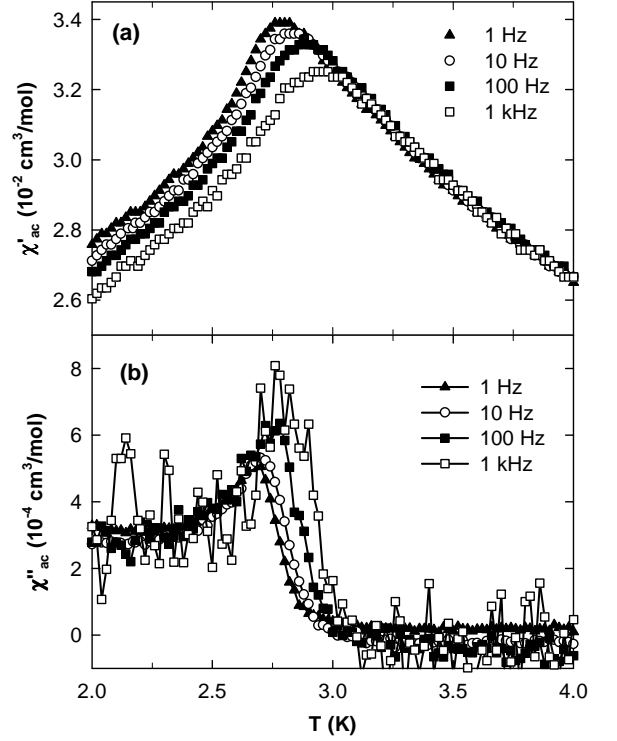


FIG. 5: (a) The real part of the ac magnetic susceptibility χ'_{ac} versus temperature T data between 2 K and 4 K for In_2VO_5 measured with various drive frequencies. (b) The imaginary part of the ac magnetic susceptibility χ''_{ac} data shown in (a) versus temperature T .

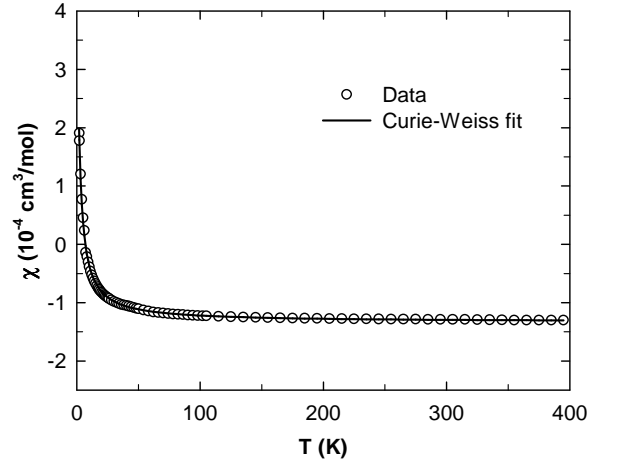


FIG. 6: The magnetic susceptibility χ versus temperature T for In_2TiO_5 measured with an applied magnetic field of 2 T. the solid curve through the data is a fit by the Curie-weiss law.

C. Heat Capacity

The heat capacity C versus temperature T of In_2VO_5 and In_2TiO_5 between 1.8 K and 300 K is shown in Fig. 7(a). There is no obvious anomaly in the $C(T)$ data

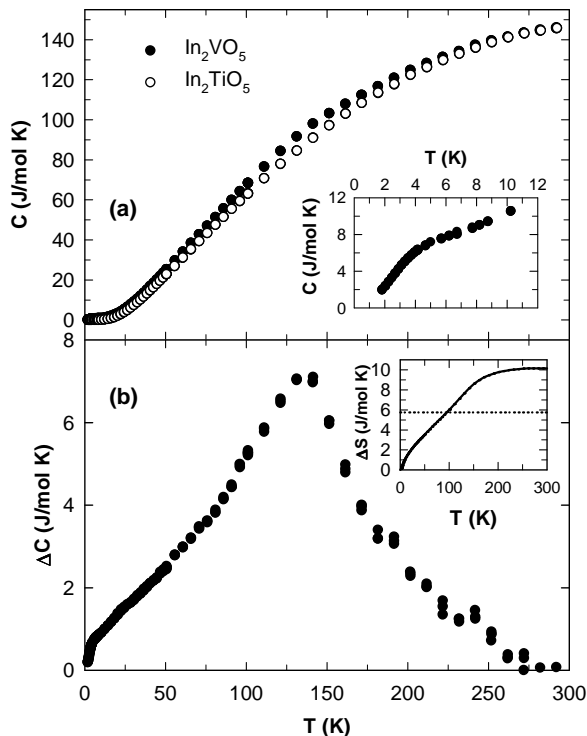


FIG. 7: (a) The heat capacity C versus temperature T for In_2VO_5 and In_2TiO_5 . The inset in (a) shows the C data between 1.8 K and 10 K to highlight the anomaly at 2.8 K. (b) The difference ΔC between the heat capacities of In_2VO_5 and In_2TiO_5 . The inset in (b) shows the difference entropy ΔS (solid curve) versus T obtained by integrating $\Delta C/T$ versus T . The dotted line corresponds to the value $\Delta S = R \ln 2 = 5.67$ J/mol K expected for $S = 1/2$ moments.

for In_2VO_5 either at 150 K where the deviation in $\chi(T)$ from the Curie-Weiss behavior was observed, or at 2.8 K where the cusp in the low field χ data was observed. The inset in Fig. 7(a) shows the C data for In_2VO_5 between 1.8 K and 10 K showing the weak shoulder with a maximum at about 5 K. A broad anomaly with a maximum at a slightly higher temperature than the temperature T_f of the cusp observed in the χ data is also a feature observed for a spin-glass transition.¹³ Figure 7(b) shows ΔC versus T , obtained by subtracting the heat capacity of In_2TiO_5 from that of In_2VO_5 . The ΔC shows a broad anomaly with a well defined maximum at about 130 K. A significant ΔC spread over the whole temperature range suggests the presence of short range magnetic interactions. However, the relatively sharp feature in ΔC at ≈ 130 K is in contrast to the gradual change in the $\chi(T)$ data below this temperature. This indicates that the anomaly in ΔC is at least not entirely of magnetic origin. The inset in Fig. 7(b) shows the difference entropy ΔS versus T (solid curve) obtained by integrating the $\Delta C/T$ versus T data. The horizontal dotted line corresponds to the value $R \ln 2 = 5.67$ J/mol K expected for disordered $S = 1/2$ moments. The ΔS at 300 K exceeds $R \ln 2$ by 75% which indicates that the whole $\Delta C(T)$ can-

not be accounted for just by magnetism, and that the anomaly at 130 K in ΔC arises from a lattice change of some kind.

The $C(T)$ data of the nonmagnetic compound In_2TiO_5 between 1.8 K and 10 K could be fitted by the expression $C = \beta T^3$ for the lattice heat capacity and gave the value $\beta = 0.100(1)$ mJ/mol K⁴. From the value of β one can obtain the Debye temperature θ_D using the expression¹⁵

$$\Theta_D = \left(\frac{12\pi^4 R n}{5\beta} \right)^{1/3}, \quad (1)$$

where R is the molar gas constant and n is the number of atoms per formula unit ($n = 8$ for In_2TiO_5). We obtain $\Theta_D = 539(2)$ K for In_2TiO_5 . The low temperature $C(T)$ of In_2VO_5 could not be used to obtain θ_D because of the presence of the shoulder at 5 K.

IV. DISCUSSION

Our data have revealed unusual magnetic and thermal properties of the $S = 1/2$ zig-zag spin-chain compound In_2VO_5 . High temperature $\chi(T)$ data indicate that there are predominantly ferromagnetic interactions between the V^{4+} moments. However, there is no signature of long-range magnetic ordering for the compound down to 1.8 K. Instead a spin-glass state is indicated below 3 K which in turn suggests the presence of atomic or magnetic disorder and frustrating interactions in the system at this temperature. The $S = 1/2$ zig-zag spin-chain model with ferromagnetic and antiferromagnetic exchange interactions J_1 and J_2 has recently been investigated and the susceptibility versus temperature, magnetization versus magnetic field and heat capacity versus temperature are reported for various values of J_1 and J_2 .^{16,17} Our $\chi(T)$, $M(H)$ and $C(T)$ data cannot be fitted consistently by these models for any value of the parameters J_1 and J_2 . For example, from Fig. 3 in Ref. 17, for the case of ferromagnetic nearest-neighbor interaction J_1 and antiferromagnetic next-nearest-neighbor interaction J_2 , a maximum in χ is predicted at $T/J_1 = 0.02$ for $J_2 = -0.28J_1$ to $-0.4J_1$. The χ data for In_2VO_5 in Fig. 4 can be qualitatively explained by the prediction with $J_1 = 100$ –150 K. However, the $C(T)$ and $C(T)/T$ calculated in Ref. 17 for these values of J_1 and J_2 show a behavior at low temperatures which is not observed for In_2VO_5 in Fig. 7. The $M(H)$ calculated in Ref. 17 shows a positive curvature at low H before saturating at high H which is also qualitatively different from the $M(H)$ that we observe in Fig. 3.

The well defined anomaly in $\Delta C(T)$ at 130 K in Fig. 7 and the large entropy difference ΔS above expectation for $S = 1/2$ moments together suggest a structural change, a strong magnetoelastic coupling and/or different lattice dynamics of the two materials In_2VO_5 and In_2TiO_5 near this temperature.

V. CONCLUSION

We have synthesized polycrystalline samples of the compounds In_2VO_5 and In_2TiO_5 and studied their structural, magnetic and thermal properties. Our results for In_2VO_5 indicate predominantly ferromagnetic exchange interactions between V^{4+} moments above 150 K. There is no signature of long-range magnetic ordering down to 1.8 K. The $\chi(T)$ data, $\chi_{ac}(T)$ at various frequencies and the $C(T)$ data all suggest that In_2VO_5 undergoes a transition into a spin-glass state below about 3 K. This in turn suggests the presence of lattice and magnetic disorder and frustration in the material. The difference ΔC between the heat capacities of In_2VO_5 and In_2TiO_5 shows a well defined peak at 130 K and the entropy difference ΔS obtained by integrating the $\Delta C/T$ versus T data up to 300 K is much larger than the value expected for $S = 1/2$ moments. The peak in ΔC and the extra entropy suggest that a structural change may occur in In_2VO_5 below 130 K, which in turn could change the V-V interactions.

Note added: After completion of this work, two preprints appeared^{18,19} on the experimental study of In_2VO_5 and both In_2VO_5 and In_2TiO_5 respectively. Reference 18 reports on the structural, magnetization, electrical resistivity and nuclear- and electron spin resonance measurements on In_2VO_5 . The value of the magnetic susceptibility χ at 1.8 K for In_2VO_5 reported in this preprint is about half of what we observe for our sample. Low temperature X-ray data show an anomalous expansion in the a and b lattice parameters below 120 K. Their ^{51}V NMR measurements show a peak at 20 K in the nuclear re-

laxation rate $1/T_1$ versus T data which they ascribe to a slowing down of spin fluctuations below this temperature. They do not observe any signature in their measurements of the spin-glass state around 3 K as we infer from our data. Reference 19 reports on the magnetic susceptibility, heat capacity and synchrotron powder x-ray diffraction measurements on In_2VO_5 and heat capacity measurements on In_2TiO_5 . The reported value of χ for In_2VO_5 at 1.8 K is consistent with our results. They observe a peak in their χ data below 3 K and ascribe it to freezing of spin dimers into a singlet state below the temperature of the maximum in χ . Their low temperature synchrotron X-ray data show an anomalous expansion in the b lattice parameters below 125 K.

The qualitative behavior of the χ reported in Refs. 18, 19 is consistent with our observations. The well-defined anomaly in the $\Delta C(T)$ that we observe at 130 K is in contrast with the subtle (less than 0.5%) variation of the lattice parameters below this temperature reported in these two preprints. Evidence of the spin-glass state below 3 K in our data is not reported in these preprints. We do not think that the ground state of In_2VO_5 is a spin-singlet as suggested in Ref. 19, because our data indicate a spin-glass ground state.

A consistent understanding of the physical properties of In_2VO_5 has not yet been reached and further experimental study will be required.

Acknowledgments

Work at the Ames Laboratory was supported by the Department of Energy-Basic Energy Sciences under Contract No. DE-AC02-07CH11358.

-
- ¹ J. G. Bednorz and K. A. Muller, Z. Phys. B **64**, 188 (1986).
 - ² M. Hase, I. Terasaki, and K. Uchinokura, Phys. Rev. Lett. **70** 3651 (1993).
 - ³ M. Azuma, Z. Hiroi, M. Takano, K. Ishida, and Y. Kitaoka, Phys. Rev. Lett. **73**, 3463 (1994).
 - ⁴ J. Darriet and R. P. Regnault, Solid State Commun. **86**, 409 (1993).
 - ⁵ E. Dagotto and T. M. Rice, Science **271**, 618 (1996).
 - ⁶ K. Kodama, M. Takigawa, M. Horvati, C. Berthier, H. Kageyama, Y. Ueda, S. Miyahara, F. Becca, and F. Mila, Science **298**, 395 (2002).
 - ⁷ G. Cao, V. Durairaj, S. Chikara, S. Parkin, and P. Schlottmann Phys. Rev. B **75**, 134402 (2007).
 - ⁸ S. Takeshita, J. Arai, T. Goko, K. Nishiyama, and K. Nagamine, J. Phys. Soc. Japan **75**, 034712 (2006).
 - ⁹ I. M. Volkova, J. Phys.: Condens. Matter **19**, 176208 (2007).
 - ¹⁰ J. Senegas, J. P. Manaud, and J. Galy, Acta Cryst **B31**, 1614 (1975).
 - ¹¹ U. Schwingenschlogl, Phys. Rev. B **75**, 212408 (2007).
 - ¹² Rietveld analysis program DBWS-9807a release 27.02.99,

- ©1998 by R. A. Young, an upgrade of “DBWS-9411 - an upgrade of the DBWS programs for Rietveld Refinement with PC and mainframe computers, R.A. Young, J. Appl. Cryst. **28**, 366 (1995)”.
- ¹³ K. H. Fisher and J. A. Hertz, *Spin Glasses* (Cambridge University Press, Cambridge, 1991).
- ¹⁴ P. W. Selwood, *Magnetochemistry*, 2nd ed. (Interscience, New York, 1956).
- ¹⁵ C. Kittel, *Solid State Physics* (John Wiley and Sons, Inc., New York, 1966).
- ¹⁶ F. Heidrich-Meisner, A. Honecker, and T. Vekua, Phys. Rev. B **74**, 020403(R) (2006).
- ¹⁷ H. T. Lu, Y. J. Wang, Shaojin Qin, and T. Xiang, Phys. Rev. B **74**, 134425 (2006).
- ¹⁸ A. Moller, T. Taetz, N. Hollmann, J.A. Mydosh, V. Kataev, M. Yehia, E. Vavilova, and B. Buchner, arXiv:0708.2088 (2007).
- ¹⁹ Simon A. J. Kimber, Mark A. de Vries, Javier Sanchez-Benitez, Konstantin V. Kamenev, and J. Paul Attfield, arxiv:0708.2550 (2007).